Dolabellanes with Antibacterial Activity from the Brown Alga *Dilophus spiralis*

Efstathia Ioannou,[†] Antonio Quesada,[‡] M. Mukhlesur Rahman,[§] Simon Gibbons,[§] Constantinos Vagias,[⊥,†] and Vassilios Roussis*,[†]
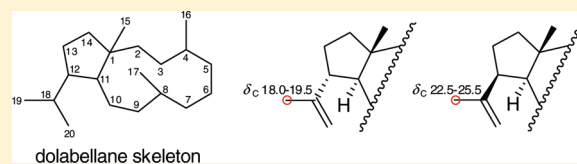
[†]Department of Pharmacognosy and Chemistry of Natural Products, School of Pharmacy, University of Athens, Panepistimiopolis Zografou, Athens 15771, Greece

[‡]Department of Didactics of Sciences, University of Jaén, PO 23071, Jaén, Spain

[§]Department of Pharmaceutical and Biological Chemistry, School of Pharmacy, University of London, 29-39 Brunswick Square, London WC1N 1AX, U.K.

ⓢ *Supporting Information*

ABSTRACT: Seventeen diterpenes featuring the dolabellane skeleton (**1**−**17**) were isolated from the organic extracts of the brown alga *Dilophus spiralis*. Seven compounds are new natural products (**1, 3, 5, 6, 11, 14, 15**) and eight are structurally revised (**2, 4, 7**−**10, 12, 13**), among which three are reported for the first time from a natural source (**4, 9, 10**). The structure elucidation and the assignment of the relative configurations of the isolated natural products were based on detailed analyses of their spectroscopic data. The structure of metabolite **10** was confirmed by single-crystal X-ray diffraction analysis, whereas the absolute configurations of compounds **2, 4**−**10, 12**, and **13** were determined using the modified Mosher's method on the semisynthetic product **18** and chemical interconversions. The antibacterial activities of compounds **1**−**18** were evaluated against six strains of *Staphylococcus aureus*, including multidrug- and methicillin-resistant variants.
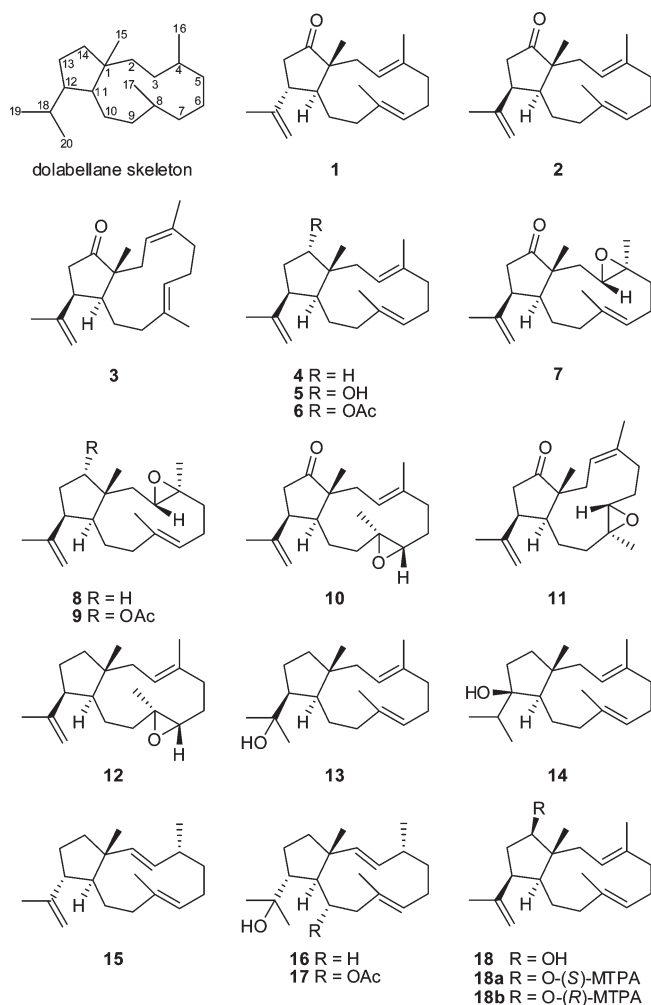
dolabellane skeleton

■ RESULTS AND DISCUSSION

Specimens of the brown alga *D. spiralis*, collected on Elafonissos Island, Greece, were exhaustively extracted with CH₂Cl₂

Brown algae of the family Dictyotaceae are widely distributed in the tropical and subtropical waters of the world, found mainly in the Atlantic, Pacific, and Indian Oceans, the Caribbean and Mediterranean Seas, and the Sea of Japan. They have been the subject of extensive studies in the last five decades, having yielded almost 500 new secondary metabolites to date. The majority of these natural products are sesquiterpenes and diterpenes of normal or mixed biosynthesis, often exhibiting antibacterial, antiviral, cytotoxic, algicidal, antifouling, antifeedant, and/or ichthyotoxic activity.[1,2]

In the course of our continuing research aimed at the isolation of bioactive natural products from marine organisms found along the coastlines of Greece, we undertook a thorough investigation of the chemical composition of *Dilophus spiralis* (Montagne) Hamel (syn. *ligulatus*). Previously, we reported the isolation and structural characterization of five new dolastanes, one new 2,6-*cyclo*-xenicane, and several known metabolites from *D. spiralis*.[3,4] Herein, we describe the isolation and structure elucidation of 17 dolabellanes (**1**−**17**) from the same algal specimens and the evaluation of their antibacterial activities against six strains of *Staphylococcus aureus*, some of which are resistant, via multidrug efflux. Seven compounds are new natural products (**1, 3, 5, 6, 11, 14, 15**) and eight are structurally revised (**2, 4, 7**−**10, 12, 13**), among which three are reported for the first time from a natural source (**4, 9, 10**).

and MeOH, and the organic extracts were subsequently subjected to a series of chromatographic separations to allow for the isolation of compounds **1**−**17**.

Compounds **1**−**3**, isolated as oils, displayed molecular ion peaks at *m/z* 286 (EIMS), corresponding to C₂₀H₃₀O. The absorption band at 1735 cm⁻¹ in their IR spectra indicated the presence of a carbonyl group, while their ¹³C NMR spectra revealed 20 carbon signals, which were assigned to five quaternary carbon atoms, four methines, seven methylenes, and four methyls, as determined by DEPT experiments. The structural elements displayed in the ¹H and ¹³C NMR spectra of **1**−**3** (Tables 1 and 2) included four methyl groups on quaternary carbons ($\delta_{H/C}$ 0.91/17.5, 1.48/15.8, 1.54/18.1, and 1.77/18.2 for **1**; $\delta_{H/C}$ 1.09/18.3, 1.51/15.7, 1.53/16.5, and 1.70/22.8 for **2**; $\delta_{H/C}$ 0.93/21.9, 1.66/23.5, 1.63/17.2, and 1.76/25.0 for **3**), one 1,1-disubstituted double bond ($\delta_{H/C}$ 4.81, 4.93/113.5, δ_C 144.7 for **1**; $\delta_{H/C}$ 4.64, 4.91/112.1, δ_C 144.7 for **2**; $\delta_{H/C}$ 4.58, 4.91/113.3, δ_C 148.0 for **3**), two trisubstituted double bonds ($\delta_{H/C}$ 4.70/122.8, δ_C 134.6 and $\delta_{H/C}$ 4.86/125.3, δ_C 136.1 for **1**; $\delta_{H/C}$ 5.12/122.8, δ_C 136.6 and $\delta_{H/C}$ 4.84/128.3, δ_C 133.0 for **2**; $\delta_{H/C}$ 4.69/122.4, δ_C 137.4 and $\delta_{H/C}$ 5.13/125.4, δ_C 134.9 for **3**), and a ketone functionality (δ_C 221.8 for **1**; δ_C 222.8 for **2**; δ_C 226.3 for **3**). Because the carbonyl group and the three carbon−carbon double bonds accounted for four of the six degrees of unsaturation,

dolabellane skeleton   1   2

3   4 R = H / 5 R = OH / 6 R = OAc   7

8 R = H / 9 R = OAc   10   11

12   13   14

15   16 R = H / 17 R = OAc   18 R = OH / 18a R = O-(S)-MTPA / 18b R = O-(R)-MTPA

the molecular structures of **1−3** were determined as bicyclic. Analyses of their 2D NMR spectra resulted in the establishment of the same planar structure, suggesting that the three compounds were stereoisomers. Specifically, the long-range coupling between H_3-19 and H_2-20 observed in the COSY spectrum indicated the presence of an isopropenyl group, whereas the correlations of C-18 with H-12 and H_3-19, as well as of C-12 with H_3-19 and H_2-20 in the HMBC spectrum, fixed its position. The cross-peaks of H-11/H-12 and H-12/H_2-13 observed in the COSY spectrum, in combination with the HMBC correlations of C-1, C-12, and C-14 with H-11 and H_2-13, identified the five-membered ring. Furthermore, the correlations of C-3 and C-4 with H_2-2, H_2-5, and H_3-16, of C-7 and C-8 with H_2-6, H_2-9, and H_3-17, and of C-1 and C-11 with H_2-2 and H_2-10 displayed in the HMBC spectrum, in conjunction with the COSY correlations of H_2-2/H-3, H_2-5/H_2-6, H_2-6/H-7, H_2-9/H_2-10, and H_2-10/H-11, concluded the assignment of the 11-membered ring. Finally, the HMBC correlations of H_3-15 with C-1, C-11, and C-14 placed the aliphatic methyl on C-1. The relative configurations of the stereogenic centers and the geometries of the double bonds of metabolites **1−3** were assigned on the basis of interactions observed in their NOESY spectra. The NOE enhancements of H-11/H_3-19, H-12/H_3-15, H-12/H-20β, and H_3-19/H-20α evident in the NOESY spectrum of **1** suggested the *trans* fusion of the two rings and indicated that H-12 was *trans*- and *cis*-oriented relative to H-11 and H_3-15, respectively. The geometries of the Δ^3 and

Δ^7 double bonds were determined as 3*E*,7*E* on the basis of the NOE interactions of H-2α/H_3-16, H-2β/H-3, H-3/H_3-15, H-7/H-9β, and H-9α/H_3-17. This was further supported by the fact that C-16 and C-17 resonated at lower frequencies (δ_C 15.8 and 18.1, respectively). In contrast, the intense NOE enhancement of H-11/H-12 displayed in the NOESY spectra of **2** and **3**, in conjunction with the observed NOE cross-peaks of H-2α/H-11, H-2β/H_3-15, H-12/H-20α, and H_3-19/H-20β for **2** and of H-3/H-11, H-3/H-13α, H-12/H-13α, H-12/H_3-19, H-13β/H-20β, H_3-15/H-20β, and H_3-19/H-20α for **3**, suggested the *trans* fusion of the two rings and the *cis*- and *trans*-orientation of H-12 in relation to H-11 and H_3-15, respectively. The geometries of the Δ^3 and Δ^7 double bonds in **2** were determined as 3*E*,7*E* on the basis of the NOE interactions of H-2α/H_3-16, H-2α/H_3-17, H-2β/H-3, H-3/H-7, and H-3/H_3-15, as in the case of **1**, which was further supported by the fact that C-16 and C-17 resonated at lower frequencies (δ_C 15.7 and 16.5, respectively). However, the geometries of the Δ^3 and Δ^7 double bonds in **3** were determined as *Z* and *E*, respectively, on the basis of the NOE cross-peaks of H-3/H_3-16, H_2-6/H_3-17, H-7/H-9β, H-7/H-10β, and H-10β/H_3-15. This was further verified by the fact that C-16 and C-17 resonated at higher (δ_C 23.5) and lower (δ_C 17.2) frequencies, respectively. On the basis of the above-mentioned data, metabolite **1** was identified as (1*R*,3*E*,7*E*,11*S*,12*R*)-14-oxo-3,7,18-dolabellatriene, **2** as its epimer at C-12, and **3** as the geometrical isomer of **2** at Δ^3. The spectroscopic and physical characteristics of **2** were identical to those of a previously reported dolabellane, although its structure was established as that of compound **1**.[5,6] A closer examination of the details of that work revealed that the relative configuration of C-12 had been erroneously assigned, based on rather tenuous evidence prior to the introduction of 2D NMR experiments. Possible reasons for the misassignment of the relative configuration of C-12 might include a misinterpretation of the results of the lanthanide-induced shift experiments used to determined the relative orientation of H_3-15 and the isopropenyl group and the fact that the relative orientation of H-11 and H-12 was established on the basis of their coupling constant alone without the use of NOE correlations.

Compound **4**, obtained as a yellowish oil, displayed a profile closely resembling those of metabolites **1−3**. Its spectroscopic and physical characteristics were the same as those of a semisynthetic product reported in the literature, whose structure had been mistakenly assigned, concerning the relative configuration of C-12, on the basis of the original misassignment regarding compound **2**.[7] Indeed, the NOE enhancements of H-2α/H-11, H-2β/H_3-15, H-11/H-12, H-12/H-20α, and H_3-19/H-20β, as in the case of **2**, suggested the *trans* fusion of the two rings and indicated that H-12 was *cis*- and *trans*-oriented relative to H-11 and H_3-15, respectively. Thus, metabolite **4** was identified as the 14-deoxo derivative of **2**, reported for the first time as a natural product.

Compound **5**, isolated as a colorless oil, had the molecular formula $C_{20}H_{32}O$, as calculated from the HRFABMS measurements. Analysis of the spectroscopic data of **5** (Tables 1 and 2) showed a high degree of similarity with metabolite **4**. In agreement with the molecular formula, it was clear that the difference was the presence of one hydroxy group. This was verified from the signals of an oxygenated methine ($\delta_{H/C}$ 3.90/81.8) evident in the ^{1}H and ^{13}C NMR spectra, as well as the absorption band at 3370 cm^{-1} in the IR spectrum. The hydroxy group was placed at C-14 due to the heteronuclear correlations of C-14 with H-11, H-12, H_2-13, and H_3-15. The relative configurations of the stereogenic centers C-1, C-11, and C-12 and the geometries of

Table 1. ^{1}H NMR Data (400 MHz, CDCl$_3$) of Compounds 1, 3−6, and 18

position		1 (J in Hz)	3 (J in Hz)		4 (J in Hz)		5 (J in Hz)		6 (J in Hz)		18 (J in Hz)
2	α	2.35, dd (14.6, 6.6)	1.95, m	α	2.19, m	α	2.23, m	α	2.30, m	α	2.10, m
	β	1.93, dd (14.6, 6.6)		β	1.67, m	β	1.72, m	β	1.66, m	β	1.79, m
3		4.70, dd (6.6, 6.6)	4.69, dd (11.6, 2.9)		5.13, dd (11.4, 4.4)		5.10, dd (10.8, 3.8)		5.09, dd (11.1, 4.0)		5.09, dd (8.4, 6.4)
5	a	2.08, m	a 2.29, m	a	2.22, m	a	2.19, m	a	2.21, m		2.12, m
	b	2.01, m	b 1.78, m	b	2.05, m	b	2.05, m	b	2.08, m		
6	a	2.17, m	2.19, m	a	2.28, m	a	2.28, m	a	2.27, m	a	2.22, m
	b	2.11, m		b	2.03, m	b	2.03, m	b	2.05, m	b	2.08, m
7		4.86, dd (7.5, 7.5)	5.13, dd (7.7, 7.7)		4.84, m		4.87, dd (10.8, 1.8)		4.86, m		4.83, dd (9.8, 4.2)
9	α	2.03, m	α 2.15, m	a	2.11, m	a	2.10, m	a	2.11, m	a	2.05, m
	β	1.75, m	β 1.80, m	b	1.88, m	b	1.77, m	b	1.85, m	b	1.87, m
10	a	1.49, m	α 1.62, m	a	1.31, m	a	1.34, m	a	1.33, m	a	1.36, m
	b	1.37, m	β 1.18, m	b	1.23, m	b	1.23, m	b	1.22, m	b	1.18, m
11		1.99, m	2.55, ddd (8.9, 7.9, 1.5)		1.74, m		1.93, m		1.92, m		1.84, m
12		2.53, ddd (11.3, 11.3, 7.9)	2.87, dd (8.9, 8.9)		2.61, ddd (10.0, 6.8, 6.8)		2.90, ddd (9.9, 7.6, 7.6)		2.85, ddd (9.5, 7.4, 7.4)		2.56, ddd (12.4, 7.8, 6.4)
13	a	2.36, dd (18.5, 7.9)	α 2.31, dd (18.2, 8.9)	a	1.64, m	a	1.95, m	a	2.02, m	α	1.99, ddd (12.4, 6.4, 6.4)
	b	2.23, dd (18.5, 11.3)	β 2.48, d (18.2)	b	1.56, m	b	1.65, m	b	1.64, m	β	1.64, ddd (12.4, 12.4, 9.8)
14				a	1.52, m		3.90, dd (6.3, 6.3)		4.91, dd (6.0, 4.2)		3.72, dd (9.8, 6.4)
				b	1.42, m						
15		0.91, s	0.93, s		1.06, s		1.03, s		1.10, s		0.96, s
16		1.48, s	1.66, s		1.51, s		1.52, s		1.52, s		1.50, s
17		1.54, s	1.63, s		1.51, s		1.53, s		1.51, s		1.49, s
19		1.77, s	1.76, s		1.70, s		1.70, s		1.72, s		1.71, s
20	α	4.81, brs	α 4.91, brs	α	4.64, brs	α	4.63, brs	α	4.64, brs	α	4.68, brs
	β	4.93, brs	β 4.58, brs	β	4.82, brs	β	4.82, brs	β	4.85, brs	β	4.87, brs
OAc										2.03, s	

the double bonds at C-3 and C-7 were established by analysis of the key correlations displayed in the NOESY spectrum of **5**, in accordance with those of **4**. The NOE enhancements of H-2β/H-14 and H-14/H$_3$-15 suggested a *cis*-relationship between H-14 and H$_3$-15 and determined the relative configuration of C-14 as S*. Therefore, metabolite **5** was identified as the 14S-hydroxy derivative of **4**.

Compound **6**, with the molecular formula C$_{22}$H$_{34}$O$_2$, as deduced from the HRFABMS measurements, was obtained as a colorless oil. Its ^{1}H and ^{13}C NMR spectra (Tables 1 and 2) were rather similar to those of **5**, with the most prominent difference being the replacement of the hydroxy group by an acetoxy group. The shift of H-14 to higher frequencies (δ_H 4.91), in conjunction with the presence of an acetoxy group, as suggested by an ester carbonyl (δ_C 171.0) and an acetoxy methyl ($\delta_{H/C}$ 2.03/21.2), was indicative of the acetylation of the hydroxy group at C-14. The correlations observed in the homo- and heteronuclear experiments supported the proposed structure of **6** as the acetyl derivative of **5**. The relative configuration and the geometry of the double bonds of **6**, found in accordance with those of **5**, were established by analysis of its NOESY spectrum.

Compounds **7**−**9**, obtained as oils, exhibited spectroscopic and physical characteristics consistent with those of dolabellanes already reported in the literature, whose structures had been incorrectly assigned, concerning the relative configuration of C-12, on the basis of the original misassignment regarding compound **2**.[5,6] Inspection of the NOESY spectra of **7**−**9** revealed cross-peaks of H-2α/H-12, H-2β/H-3, H-3/H$_3$-15, H-11/H-12, H-12/H-20α, and H$_3$-19/H-20β, thus determining the same relative configurations for C-1, C-11, and C-12 as in **2**−**6**. Metabolite **9** is reported for the first time as a natural product.

Compounds **10** and **11**, isolated as white crystals and a colorless oil, respectively, displayed molecular ion peaks at m/z 302 (EIMS), corresponding to C$_{20}$H$_{30}$O$_2$. The structural elements displayed in the ^{1}H and ^{13}C NMR spectra of **10** and **11** (Tables 3 and 4) exhibited a high degree of similarity with those of metabolite **7**. In agreement with the molecular formula, it was obvious that they were both isomers of the latter. Analyses of their 2D NMR spectra resulted in the establishment of the same planar structure, implying that **10** and **11** were stereoisomers. In this case, the trisubstituted double bond remained between carbons C-3 and C-4, as in **1**−**3**, whereas the epoxide function was placed between carbons C-7 and C-8, on the basis of the HMBC correlations of C-5, C-6, C-8, and C-9 with H-7 and both C-7 and C-8 with H$_2$-6, H$_2$-9, and H$_3$-17. The relative configuration and the geometry of the double bond of both metabolites were assigned on the basis of interactions observed in their NOESY spectra. The intense NOE enhancement of H-11/H-12 established the same relative

Table 2. ^{13}C NMR Data (50 MHz, CDCl$_3$) of Compounds 1, 3−6, and 18

position	1		3		4		5		6		18	
1	53.0,	C	50.6,	C	46.5,	C	48.3,	C	49.2,	C	48.9,	C
2	35.2,	CH$_2$	38.0,	CH$_2$	43.4,	CH$_2$	35.0,	CH$_2$	35.2,	CH$_2$	40.0,	CH$_2$
3	122.8,	CH	122.4,	CH	125.8,	CH	124.2,	CH	124.4,	CH	124.5,	CH
4	134.6,	C	137.4,	C	134.5,	C	135.4,	C	135.4,	C	134.9,	C
5	39.3,	CH$_2$	31.7,	CH$_2$	39.9,	CH$_2$	39.9,	CH$_2$	39.8,	CH$_2$	39.8,	CH$_2$
6	25.0,	CH$_2$	25.2,	CH$_2$	24.4,	CH$_2$	24.4,	CH$_2$	24.9,	CH$_2$	24.6,	CH$_2$
7	125.3,	CH	125.4,	CH	127.3,	CH	126.8,	CH	127.3,	CH	127.2,	CH
8	136.1,	C	134.9,	C	133.9,	C	134.4,	C	133.9,	C	134.1,	C
9	37.1,	CH$_2$	36.0,	CH$_2$	37.7,	CH$_2$	36.8,	CH$_2$	37.3,	CH$_2$	38.2,	CH$_2$
10	29.9,	CH$_2$	23.8,	CH$_2$	24.4,	CH$_2$	26.3,	CH$_2$	24.4,	CH$_2$	24.1,	CH$_2$
11	43.3,	CH	41.7,	CH	41.8,	CH	42.0,	CH	41.8,	CH	41.4,	CH
12	49.9,	CH	41.4,	CH	51.0,	CH	46.0,	CH	47.1,	CH	44.4,	CH
13	42.0,	CH$_2$	47.1,	CH$_2$	28.5,	CH$_2$	37.6,	CH$_2$	35.0,	CH$_2$	37.7,	CH$_2$
14	221.8,	C	226.3,	C	42.1,	CH$_2$	81.8,	CH	83.3,	CH	80.3,	CH
15	17.5,	CH$_3$	21.9,	CH$_3$	24.3,	CH$_3$	22.3,	CH$_3$	22.6,	CH$_3$	16.9,	CH$_3$
16	15.8,	CH$_3$	23.5,	CH$_3$	15.6,	CH$_3$	15.5,	CH$_3$	15.6,	CH$_3$	15.7,	CH$_3$
17	18.1,	CH$_3$	17.2,	CH$_3$	16.7,	CH$_3$	17.7,	CH$_3$	17.0,	CH$_3$	16.4,	CH$_3$
18	144.7,	C	148.0,	C	146.9,	C	146.4,	C	145.7,	C	145.6,	C
19	18.2,	CH$_3$	25.0,	CH$_3$	23.5,	CH$_3$	23.3,	CH$_3$	23.3,	CH$_3$	23.3,	CH$_3$
20	113.5,	CH$_2$	113.3,	CH$_2$	111.2,	CH$_2$	112.4,	CH$_2$	112.2,	CH$_2$	112.1,	CH$_2$
OAc									171.0,	C		
OAc									21.2,	CH$_3$		

Table 3. ^{1}H NMR Data (400 MHz, CDCl$_3$) of Compounds 9−11 and 13−15

position		9 (J in Hz)		10 (J in Hz)		11 (J in Hz)		13 (J in Hz)		14 (J in Hz)		15 (J in Hz)
2	α	1.41, dd (14.2, 11.0)	α	2.15, m		2.15, m	a	2.11, m	a	2.09, m		5.20, d (15.9)
	β	1.78, dd (14.2, 2.4)	β	1.83, dd (13.1, 3.9)			b	1.67, m	b	1.73, m		
3		2.89, dd (11.0, 2.4)		5.38, dd (11.4, 3.9)		4.73, m		4.98, dd (7.2, 7.2)		4.93, m		5.13, dd (15.9, 7.8)
4												2.03, m
5	α	2.14, m		2.27, m	a	2.53, m		2.08, m		2.08, m	a	1.52, m
	β	1.24, m			b	1.88, dd (14.0, 7.4)					b	1.34, m
6	α	2.32, m	α	1.56, m	a	2.03, m	a	2.13, m	a	2.14, m	a	2.12, m
	β	2.16, m	β	1.90, m	b	1.44, m	b	2.10, m	b	2.10, m	b	2.08, m
7		5.03, brd (10.7)		2.72, brd (10.0)		2.88, m		4.86, dd (6.7, 6.7)		4.95, m		4.98, dd (9.8, 5.4)
9	α	2.00, m	α	2.01, m	a	2.02, m		2.12, m	a	2.11, m	α	1.99, m
	β	2.19, m	β	1.28, m	b	1.55, m			b	1.83, m	β	1.57, m
10	a	1.39, m		1.42, m	α	1.51, m		1.50, m	a	1.64, m	a	1.42, m
	b	1.28, m			β	1.37, m			b	1.27, m	b	1.23, m
11		1.95, m		2.14, m		2.52, m		1.52, m		1.67, m		1.37, m
12		2.77, ddd (11.7, 7.0, 7.0)		2.94, ddd (7.9, 7.7, 7.7)		2.89, m		1.72, m				2.27, m
13	a	2.03, m		2.40, m	a	2.54, m	a	1.65, m	a	1.68, m	a	1.76, m
	b	1.57, m			b	2.29, dd (18.4, 9.0)	b	1.33, m	b	1.42, m	b	1.50, m
14		4.84, dd (7.1, 3.2)					a	1.44, m	a	1.57, m	a	1.72, m
							b	1.37, m	b	1.43, m	b	1.41, m
15		1.29, s		1.08, s		0.96, s		0.97, s		0.97, s		0.85, s
16		1.23, s		1.64, s		1.67, s		1.54, s		1.48, s		0.91, d (6.8)
17		1.56, s		1.27, s		1.33, s		1.53, s		1.55, s		1.46, s
18										1.85, m		
19		1.70, s		1.73, s		1.79, s		1.21, s		0.93, d (6.8)		1.70, s
20	α	4.63, brs	α	4.69, brs	α	4.95, brs		1.23, s		0.97, d (6.6)	α	4.68, brs
	β	4.87, brs	β	4.96, brs	β	4.61, brs					β	4.70, brs
OAc		2.01, s										

Table 4. ^{13}C NMR Data (50 MHz, CDCl$_3$) of Compounds 9−11 and 13−15

position	9		10		11		13		14		15	
1	46.7,	C	52.8,	C	50.1,	C	46.7,	C	44.5,	C	45.1,	C
2	35.6,	CH$_2$	37.1,	CH$_2$	38.0,	CH$_2$	38.7,	CH$_2$	41.8,	CH$_2$	136.5,	CH
3	63.9,	CH	122.1,	CH	122.8,	CH	124.6,	CH	124.2,	CH	132.7,	CH
4	62.0,	C	136.9,	C	137.5,	C	133.0,	C	133.8,	C	38.5,	CH
5	38.8,	CH$_2$	37.9,	CH$_2$	27.7,	CH$_2$	39.5,	CH$_2$	39.0,	CH$_2$	35.3,	CH$_2$
6	24.2,	CH$_2$	23.6,	CH$_2$	25.1,	CH$_2$	24.9,	CH$_2$	24.3,	CH$_2$	27.8,	CH$_2$
7	126.5,	CH	64.9,	CH	62.5,	CH	126.5,	CH	124.4,	CH	127.2,	CH
8	133.8,	C	61.2,	C	62.2,	C	135.3,	C	135.9,	C	133.2,	C
9	37.1,	CH$_2$	36.2,	CH$_2$	35.0,	CH$_2$	39.2,	CH$_2$	37.7,	CH$_2$	40.5,	CH$_2$
10	23.2,	CH$_2$	23.3,	CH$_2$	23.7,	CH$_2$	31.5,	CH$_2$	23.0,	CH$_2$	24.9,	CH$_2$
11	42.0,	CH	41.9,	CH	42.5,	CH	41.7,	CH	45.6,	CH	55.1,	CH
12	47.7,	CH	43.3,	CH	40.9,	CH	60.2,	CH	87.3,	C	54.1,	CH
13	34.3,	CH$_2$	42.0,	CH$_2$	46.9,	CH$_2$	26.4,	CH$_2$	30.5,	CH$_2$	27.3,	CH$_2$
14	83.1,	CH	222.3,	C	224.7,	C	41.1,	CH$_2$	39.5,	CH$_2$	39.8,	CH$_2$
15	22.5,	CH$_3$	18.0,	CH$_3$	21.3,	CH$_3$	23.2,	CH$_3$	24.3,	CH$_3$	20.7,	CH$_3$
16	15.9,	CH$_3$	15.9,	CH$_3$	23.8,	CH$_3$	16.4,	CH$_3$	15.6,	CH$_3$	22.6,	CH$_3$
17	16.3,	CH$_3$	19.1,	CH$_3$	21.7,	CH$_3$	16.5,	CH$_3$	17.4,	CH$_3$	16.6,	CH$_3$
18	145.0,	C	144.6,	C	147.0,	C	73.3,	C	35.0,	CH	147.5,	C
19	22.8,	CH$_3$	23.4,	CH$_3$	25.2,	CH$_3$	26.5,	CH$_3$	18.7,	CH$_3$	18.5,	CH$_3$
20	112.1,	CH$_2$	113.4,	CH$_2$	114.2,	CH$_2$	30.8,	CH$_3$	17.9,	CH$_3$	110.4,	CH$_2$
OAc	170.9,	C										
OAc	21.2,	CH$_3$										

configurations for C-1, C-11, and C-12 as in **7**. The NOE interactions of H-3/H-7, H-7/H$_3$-15, H-11/H$_3$-17, and H$_3$-16/H$_3$-17 for **10** and the cross-peaks of H-7/H-10β, H-10β/H$_3$-15, H-11/H$_3$-17, and H$_3$-16/H$_3$-17 for **11** suggested that the oxygenated methine H-7 was *cis*- and *trans*-oriented relative to H$_3$-15 and H$_3$-17, respectively, and established the relative configuration of C-7 and C-8 as 7S*,8S*. The geometry of the double bond at C-3 was established as *E* in **10** on the basis of the NOE enhancements of H-2α/H$_3$-16, H-2β/H-3, and H-3/H$_3$-15, which was further supported by the fact that C-16 resonated at lower frequencies (δ_C 15.9). On the contrary, the geometry of the Δ^3 double bond was established as *Z* in **11** on the basis of the NOE enhancements of H-3/H-11 and H-3/H$_3$-16, which was further verified by the fact that C-16 resonated at higher frequencies (δ_C 23.8). Thus, the geometrical isomers **10** and **11** were identified as positional isomers of **7**. The proposed structure of **10** was confirmed by single-crystal X-ray diffraction analysis (Figure 1).[8] The spectroscopic and physical characteristics of compound **10** were identical to those of a semisynthetic product reported in the literature, whose structure had been erroneously assigned concerning the relative configuration of C-12 on the basis of the original misassignment regarding compound **2**, while the relative configurations of C-7 and C-8 were not established.[5]

Compound **12**, obtained as a yellowish oil, possessed spectroscopic and physical characteristics congruent with those of a previously reported dolabellane, whose structure had been incorrectly assigned concerning the relative configuration of C-12 due to the overlap of H-7 and H-12 and the misinterpretation thereafter of the NOE correlations observed.[9] The NOE enhancements of H-2α/H$_3$-16, H-2β/H-3, H-3/H-7, H-3/H$_3$-15, H-7/H$_3$-15, H-11/H-12, H-12/H-20α, and H$_3$-19/H-20β, more easily distinguishable in 1D NOE experiments, indicated the same relative configurations for C-1, C-7, C-8, C-11, and

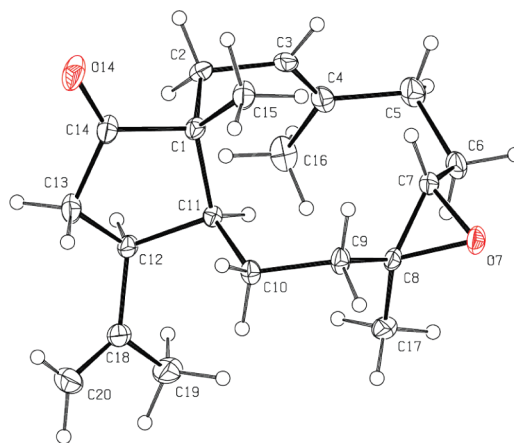**Figure 1.** ORTEP drawing of compound **10**. Displacement ellipsoids are shown at 30% probability.

C-12 and the geometry of the Δ^3 double bond as in the case of **10**.

Compound **13**, isolated as a colorless oil, displayed spectroscopic and physical characteristics identical to those of a previously reported dolabellane, whose structure had been erroneously assigned, concerning the relative configuration of C-12, on the basis of the original misassignment regarding compound **2**.[7] As in the case of metabolites **2**−**12**, the NOE enhancement of H-11/H-12 indicated the same relative configurations for C-1, C-11, and C-12.

Compound **14**, with the molecular formula $C_{20}H_{34}O$, as deduced from the HRFABMS measurements, was obtained as a colorless oil. The structural characteristics evident in the ^{1}H and ^{13}C NMR spectra included three singlet methyls ($\delta_{H/C}$ 0.97/24.3, 1.48/15.6, and 1.55/17.4), two doublet methyls

Scheme 1. Chemical Interconversions Performed[a] **Correlating Compounds 2, 4−10, 12, 13, and 18**
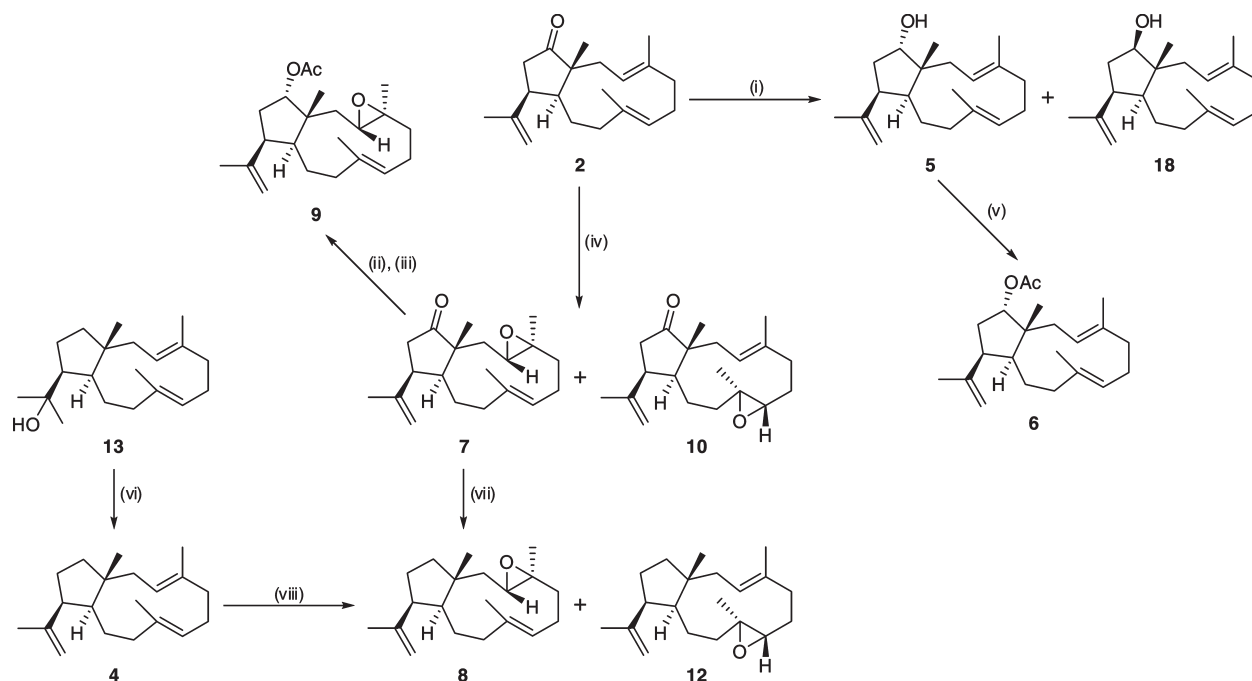
[a] Reagents and conditions: (i) NaBH$_4$, MeOH, 1 h; (ii) NaBH$_4$, EtOH, 2 h; (iii) Ac$_2$O, pyridine, overnight; (iv) m-CPBA, benzene, 45 min; (v) Ac$_2$O, pyridine, 70 °C, 16 h; (vi) POCl$_3$, pyridine, 0 °C, 20 min; (vii) N$_2$H$_4$·H$_2$O, N$_2$H$_4$·2HCl, TEG, 130 °C, 1.5 h, KOH, 170 °C, 2 h; (viii) m-CPBA, benzene, 30 min.

($\delta_{H/C}$ 0.93/18.7 and 0.97/17.9), two trisubstituted double bonds ($\delta_{H/C}$ 4.93/124.2, δ_C 133.8 and $\delta_{H/C}$ 4.95/124.4, δ_C 135.9), and an oxygenated quaternary carbon (δ_C 87.3). The spectroscopic data of **14** (Tables 3 and 4) closely resembled those of **13**. In this case, the hydroxy group was placed at C-12, as indicated by the HMBC correlations of C-12 with H-11, H$_2$-13, H$_3$-19, and H$_3$-20 and the COSY cross-peaks of H-18 with both H$_3$-19 and H$_3$-20. The geometries of the Δ^3 and Δ^7 double bonds were determined as 3E,7E due to the fact that C-16 and C-17 resonated at lower frequencies (δ_C 15.6 and 17.4, respectively). On the basis of the interaction of H-11/H$_3$-19 observed in the NOESY spectrum, measured in C$_6$D$_6$ because there was partial overlapping of key NMR signals in CDCl$_3$, the relative configurations of C-1, C-11, and C-12 were established as 1R*,11R*,12R*.

Compound **15**, obtained as a colorless oil, displayed an ion peak at m/z 272.2495 (HRFABMS), corresponding to C$_{20}$H$_{32}$ and consistent with [M]$^+$. Analysis of the spectroscopic data of **15** (Tables 3 and 4) showed a high degree of similarity with metabolite **4**, and with an identical molecular formula, it was obvious that the two were isomers. In the ^{1}H NMR spectrum three singlet methyls (δ_H 0.85, 1.46, and 1.70), one doublet methyl (δ_H 0.91), an exomethylene group (δ_H 4.68 and 4.70), and three olefinic methines (δ_H 4.98, 5.13, and 5.20) were evident, suggesting that the difference between the two molecules was the replacement of a trisubstituted double bond by a 1,2-disubstituted one. The 1,2-disubstituted double bond was placed between C-2 and C-3 on the basis of the COSY cross-peaks of H-2/H-3, H-3/H-4, H-4/H$_2$-5, and H-4/H$_3$-16 and the correlations of C-1 and C-15 with H-2, as well as of C-3, C-4, and C-5 with H$_3$-16. Inspection of the NOESY spectrum of **15** revealed the interaction of H-12/H$_3$-15, which led to the
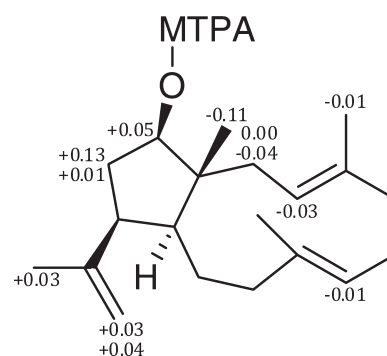

Figure 2. $\Delta\delta_{S-R}$ values (ppm) for the C-14 MTPA derivatives of **18** in CDCl$_3$.

determination of the relative configurations of C-1, C-11, and C-12 as 1R*,11S*,12R*. Furthermore, the NOE enhancements of H-2/H-11, H-2/H$_3$-16, H-11/H$_3$-17, H-3/H-7, and H-3/H$_3$-15 established the relative configuration of C-4 as R* and the geometries of the double bonds at C-2 and C-7 as 2E,7E. The latter conclusion was also supported by the large coupling constant of H-2/H-3 (15.9 Hz) and the fact that C-17 resonated at lower frequencies (δ_C 16.6).

Reduction of metabolite **2** yielded both epimeric alcohols at C-14 (**5** and **18**), while acetylation of metabolite **5** afforded **6**. Furthermore, epoxidation of metabolite **4** yielded monoepoxides **8** and **12** (Scheme 1). Semisynthetic compounds **5**, **6**, **8**, and **12** were identical in all respects to the natural products, whereas **18** was not detected as a natural product during the chromatographic separations. In the previous reports on compounds **2**, **4**, **7−10**, and **13**, several chemical interconversions were used to

Table 5. Antibacterial Activities[a] of Compounds 1−18

compound	ATCC 25923	EMRSA-15	EMRSA-16	RN4220	SA1199B	XU212
1	inactive[b]	inactive[b]	inactive[b]	inactive[b]	inactive[b]	inactive[b]
2	inactive[b]	inactive[b]	16	inactive[b]	128	inactive[b]
3	inactive[b]	inactive[b]	inactive[b]	inactive[b]	inactive[b]	inactive[b]
4	64	128	16	128	128	128
5	128	64	8	64	32	64
6	inactive[b]	inactive[b]	inactive[b]	inactive[b]	inactive[b]	inactive[b]
7	inactive[b]	inactive[b]	inactive[b]	128	inactive[b]	inactive[b]
8	inactive[b]	inactive[b]	32	inactive[b]	inactive[b]	inactive[b]
9	32	128	32	64	64	128
10	inactive[b]	inactive[b]	inactive[b]	inactive[b]	inactive[b]	inactive[b]
11	inactive[b]	inactive[b]	inactive[b]	inactive[b]	inactive[b]	inactive[b]
12	inactive[b]	128	4	inactive[b]	inactive[b]	inactive[b]
13	32	32	8	64	32	64
14	8	8	8	8	16	16
15	inactive[b]	inactive[b]	inactive[b]	inactive[b]	inactive[b]	inactive[b]
16	64	64	16	64	64	64
17	inactive[b]	inactive[b]	64	inactive[b]	inactive[b]	inactive[b]
18	4	2	2	4	2	4
norfloxacin	0.5	0.5	128	0.5	32	8

[a] Expressed as MIC (in μg/mL). [b] MIC > 128 μg/mL.

correlate them, and it was proven that the relative configurations of the asymmetric centers C-1, C-11, and C-12 remained unchanged (Scheme 1).[5,7] In the present study it was shown using the observed NOE enhancements that the relative configuration of C-12 of these compounds should be inverted, a fact that was also verified through the single-crystal X-ray diffraction analysis of 10. The absolute configuration of 18 was determined by application of a modified Mosher's method.[10] When 18 was treated with (R)- and (S)-MTPA chloride, the secondary hydroxy group at C-14 reacted to give the (S)- and (R)-MTPA derivatives (18a and 18b), respectively. The ^{1}H NMR chemical shifts of 18a and 18b were assigned by analysis of ^{1}H NMR, HSQC, and COSY spectra. The calculation of the $\Delta\delta_{S-R}$ values, shown in Figure 2, clearly defined the absolute configuration of C-14 as R and, subsequently, on the basis of its relative configuration, established the absolute configuration of 18 as depicted. Because compounds 2, 4−10, 12, 13, and 18 were clearly correlated through the chemical interconversions described above, the absolute configurations of 2, 4−10, 12, and 13 are also as shown. The absolute configurations of metabolites 1, 3, 11, 14, and 15 were not determined, but on the basis of biogenetic considerations they are expected to be the same.

In addition to metabolites 1−15, two known natural products were isolated and identified as (1R,2E,4R,7E,11S,12R)-18-hydroxy-2,7-dolabelladiene (16) and (1R,2E,4R,7E,10S,11S,12R)-10-acetoxy-18-hydroxy-2,7-dolabelladiene (17) by comparison of their spectroscopic and physical characteristics with those reported in the literature.[11] Even though the absolute configurations of 16 and 17 were not established, they are expected to be the same as those of 1−15 on the basis of a common biogenetic route. Furthermore, the ^{1}H and ^{13}C NMR chemical shifts for compounds 4, 9, 10, and 13 are presented in Tables 1−4, supplementing the relevant literature, since only a few characteristic ^{1}H NMR resonances were available.

Comprehensive examination of the spectroscopic data for compounds 1−12, 15, and 18, as well as for other previously described dolabellanes featuring an isopropenyl group,[12,13] revealed that the chemical shift of C-19 is very characteristic of the orientation of methine H-12 relative to H-11 and H$_3$-15. Specifically, when H-12 is cis- and trans-oriented in relation to H-11 and H$_3$-15, respectively, C-19 resonates at higher frequencies (δ_C 22.5 to 25.5), whereas when H-12 is trans- and cis-oriented relative to H-11 and H$_3$-15, respectively, C-19 resonates at lower frequencies (δ_C 18.0 to 19.5).

Compounds 1−18 were evaluated for their antibacterial activities against a panel of six strains of *Staphylococcus aureus*. These included a standard laboratory strain (ATCC 25923), two epidemic MRSA strains (EMRSA-15 and EMRSA-16), a macrolide-resistant variant (RN4220), and two multi-drug-resistant effluxing strains (SA1199B and XU212). According to the results of the antibacterial activity assessment (Table 5), the most active compound against all tested bacterial strains was the semisynthetic alcohol 18, with MIC values in the range 2−4 μg/mL. Interestingly, metabolite 5, which is the epimer of 18 at C-14, exhibited moderate activity against strain EMRSA-16 with a MIC value of 8 μg/mL, but only weak activity against the other strains, with MIC values ranging from 32 to 128 μg/mL. Metabolite 14 was moderately active against all tested strains, with MIC values in the range 8−16 μg/mL, while compounds 2, 4, 12, 13, and 16 displayed moderate activity only against strain EMRSA-16, with MIC values between 4 and 16 μg/mL, but weak or no activity against the other strains. Thus, it seems that strain EMRSA-16 is fairly susceptible to dolabellane diterpenes. It is worth noting that the majority of the dolabellanes that demonstrated antibacterial activity against the tested strains possessed a hydroxy group, whereas the presence of a ketone functionality at C-14 rendered the dolabellanes inactive.

■ EXPERIMENTAL SECTION

General Experimental Procedures. Optical rotations were measured on a Perkin-Elmer model 341 polarimeter with a 1 dm cell.

UV spectra were obtained on a Shimadzu UV-160A spectrophotometer. IR spectra were obtained on a Paragon 500 Perkin-Elmer spectrometer. NMR spectra were recorded on Bruker AC 200 and Bruker DRX 400 spectrometers. Chemical shifts are given on a δ (ppm) scale using TMS as internal standard. The 2D experiments (HSQC, HMBC, COSY, NOESY) were performed using standard Bruker pulse sequences. High-resolution mass spectrometric data were provided by the University of Notre Dame, Department of Chemistry and Biochemistry, Notre Dame, IN, USA. Low-resolution EI mass spectra were measured on a Hewlett-Packard 5973 mass spectrometer. Column chromatography separations were performed with Kieselgel 60 (Merck). HPLC separations were conducted using a CECIL 1100 Series liquid chromatography pump equipped with a GBC LC-1240 refractive index detector, using the following columns: (i) Spherisorb S10W (Phase Sep, 25 cm × 10 mm), (ii) Econoshpere Silica 10u (Grace, 25 cm × 10 mm), and (iii) Chiralcel OD 10 μm (Daicel Chemical Industries Ltd., 25 cm × 10 mm). TLC was performed with Kieselgel 60 F$_{254}$ (Merck aluminum support plates), and spots were detected after spraying with 15% H$_2$SO$_4$ in MeOH reagent and heating at 100 °C for 1 min. The lyophilization was carried out in a Freezone 4.5 freeze-dry system (Labconco).

Plant Material. Specimens of *Dilophus spiralis* were collected by hand on Elafonissos Island (GPS coordinates 36°30′ N, 22°58′ E), south of Peloponnese, Greece, at a depth of 0.1−1 m, in April 2004. A voucher specimen of the alga has been deposited at the Herbarium of the Department of Pharmacognosy and Chemistry of Natural Products, University of Athens (ATPH/MO/159).

Extraction and Isolation. Specimens of the freeze-dried alga (272 g) were exhaustively extracted with CH$_2$Cl$_2$ and subsequently with MeOH at room temperature. Evaporation of the solvents in vacuo afforded two dark green oily residues. The CH$_2$Cl$_2$ residue (9.2 g) was subjected to vacuum column chromatography on silica gel, using cyclohexane with increasing amounts of EtOAc, followed by EtOAc with increasing amounts of MeOH as the mobile phase, to yield 15 fractions (A1−A15). Fractions A1 (100% cyclohexane, 131.4 mg) and A2 (10% EtOAc in cyclohexane, 18.3 mg) were separately and repeatedly purified by normal-phase HPLC, using *n*-hexane (100%) as eluent, to afford **4** (39.6 mg) and **15** (0.9 mg). Fraction A3 (20% EtOAc in cyclohexane, 1.17 g) was further fractionated by gravity column chromatography on silica gel, using cyclohexane with increasing amounts of EtOAc as the mobile phase, to yield 21 fractions (A3a−A3u). Fraction A3b (1% EtOAc in cyclohexane, 355.7 mg) was subjected to gravity column chromatography on silica gel, using cyclohexane with increasing amounts of CH$_2$Cl$_2$, followed by CH$_2$Cl$_2$ with increasing amounts of EtOAc as the mobile phase, to afford 11 fractions (A3b1−A3b11). Fractions A3b8 (100% CH$_2$Cl$_2$, 55.6 mg) and A3b9 (50% EtOAc in CH$_2$Cl$_2$, 195.6 mg) were separately purified by normal-phase HPLC, using cyclohexane/EtOAc (99:1) and subsequently *n*-hexane/EtOAc (99:1) as eluent, to yield **2** (185.6 mg), **3** (2.8 mg), and **6** (1.9 mg). Fractions A3c (1% EtOAc in cyclohexane, 162.9 mg) and A3d (1% EtOAc in cyclohexane, 55.3 mg) were separately purified by normal-phase HPLC, using *n*-hexane/EtOAc (98:2 and subsequently 99:1) as eluent, to afford **1** (1.1 mg), **2** (96.5 mg), **3** (1.5 mg), **8** (29.1 mg), and **14** (0.8 mg). Fractions A3i (2% EtOAc in cyclohexane, 81.7 mg) and A3j (2% EtOAc in cyclohexane, 28.2 mg) were purified separately by normal-phase HPLC, using cyclohexane/EtOAc (95:5) as eluent, to yield **16** (21.2 mg). Fraction A3l (10% EtOAc in cyclohexane, 81.9 mg) was subjected to gravity column chromatography on silica gel, using cyclohexane with increasing amounts of EtOAc as the mobile phase, to afford 10 fractions (A3l1−A3l10). Fraction A3l6 (6% EtOAc in cyclohexane, 7.6 mg) was purified by normal-phase HPLC, using cyclohexane/EtOAc (90:10) as eluent, to yield **5** (1.4 mg). Fraction A4 (30% EtOAc in cyclohexane, 3.58 g) was further fractionated by vacuum column chromatography on silica gel, using cyclohexane with increasing amounts of EtOAc, followed by EtOAc with increasing amounts of MeOH as the mobile phase, to

afford nine fractions (A4a−A4i). Fraction A4b (10% EtOAc in cyclohexane, 46.1 mg) was purified by normal-phase HPLC, using cyclohexane/EtOAc (98:2) as eluent, to yield **1** (0.4 mg), **2** (12.8 mg), **8** (2.2 mg), **12** (0.4 mg), and **13** (1.2 mg). Fraction A4c (20% EtOAc in cyclohexane, 812.3 mg) was subjected to gravity column chromatography on silica gel, using cyclohexane with increasing amounts of EtOAc, followed by EtOAc with increasing amounts of MeOH as the mobile phase, to afford 23 fractions (A4c1−A4c23). Fractions A4c2 (1% EtOAc in cyclohexane, 174.3 mg), A4c3 (1% EtOAc in cyclohexane, 129.8 mg), and A4c4 (1% EtOAc in cyclohexane, 9.9 mg) were separately purified by normal-phase HPLC, using *n*-hexane/EtOAc (97:3) and subsequently *n*-hexane/2-propanol (99.5:0.5) as eluent, to yield **1** (1.4 mg), **2** (144.8 mg), **3** (2.7 mg), **8** (2.4 mg), and **12** (7.8 mg). Fractions A4c10 (2% EtOAc in cyclohexane, 17.0 mg), A4c11 (3% EtOAc in cyclohexane, 10.8 mg), A4c12 (5% EtOAc in cyclohexane, 18.7 mg), A4c13 (7% EtOAc in cyclohexane, 47.0 mg), A4c14 (10% EtOAc in cyclohexane, 46.6 mg), A4c15 (12% EtOAc in cyclohexane, 138.5 mg), A4c16 (20% EtOAc in cyclohexane, 13.3 mg), and A4c17 (20% EtOAc in cyclohexane, 24.7 mg) were separately purified by normal-phase HPLC, using cyclohexane/EtOAc (90:10) and subsequently *n*-hexane/2-propanol (90:10, 87:13, and 82:18) as eluent, to afford **5** (16.3 mg), **7** (27.2 mg), **9** (13.6 mg), **10** (17.6 mg), **11** (5.2 mg), and **16** (0.9 mg). The MeOH residue (32.8 g) was subjected to vacuum column chromatography on silica gel, using cyclohexane with increasing amounts of EtOAc, followed by EtOAc with increasing amounts of MeOH as the mobile phase, to yield 14 fractions (B1−B14). Fraction B1 (10% EtOAc in cyclohexane, 51.0 mg) was purified by normal-phase HPLC, using *n*-hexane (100%) as eluent, to afford **4** (13.3 mg). Fraction B3 (20% EtOAc in cyclohexane, 361.0 mg) was repeatedly purified by normal-phase HPLC, using cyclohexane/EtOAc (90:10) and subsequently *n*-hexane/2-propanol (86:14 and 83:17) as eluent, to yield **2** (3.3 mg), **5** (9.0 mg), **9** (5.4 mg), **11** (3.8 mg), **16** (2.4 mg), and **17** (0.9 mg).

(1R,3E,7E,11S,12R)-14-Oxo-3,7,18-dolabellatriene (**1**): colorless oil; $[\alpha]_D^{20}$ −76 (*c* 0.09, CHCl$_3$); UV (CHCl$_3$) λ_{max} (log ε) 245.5 (2.96) nm; IR (thin film) ν_{max} 2971, 2916, 1735, 1275 cm^{-1}; ^{1}H NMR data, see Table 1; ^{13}C NMR data, see Table 2; EIMS 70 eV *m/z* (rel int %) 286 (22), 271 (22), 253 (10), 243 (6), 228 (6), 213 (9), 203 (7), 189 (43), 175 (23), 161 (22), 147 (28), 135 (42), 121 (42), 107 (85), 91 (87), 79 (79), 67 (100), 53 (53); HRFABMS *m/z* 286.2303 [M]$^+$ (calcd for C$_{20}$H$_{30}$O, 286.2297).

(1R,3Z,7E,11S,12S)-14-Oxo-3,7,18-dolabellatriene (**3**): yellowish oil; $[\alpha]_D^{20}$ −98 (*c* 0.09, CHCl$_3$); UV (CHCl$_3$) λ_{max} (log ε) 241.8 (2.28) nm; IR (thin film) ν_{max} 2958, 2920, 1734, 1454 cm^{-1}; ^{1}H NMR data, see Table 1; ^{13}C NMR data, see Table 2; EIMS 70 eV *m/z* (rel int %) 286 (11), 271 (15), 253 (3), 243 (6), 229 (4), 217 (7), 203 (8), 189 (28), 175 (19), 163 (55), 150 (75), 135 (100), 121 (39), 107 (57), 93 (57), 81 (49), 67 (48), 55 (34); HRFABMS *m/z* 287.2366 [M + H]$^+$ (calcd for C$_{20}$H$_{31}$O, 287.2375).

(1R,3E,7E,11S,12S)-3,7,18-Dolabellatriene (**4**): yellowish oil; $[\alpha]_D^{20}$ +41.0 (*c* 0.10, CHCl$_3$); UV (CHCl$_3$) λ_{max} (log ε) 243.8 (2.57) nm; IR (thin film) ν_{max} 2930, 2854, 1645, 1454 cm^{-1}; ^{1}H NMR data, see Table 1; ^{13}C NMR data, see Table 2; EIMS 70 eV *m/z* (rel int %) 272 (38), 257 (26), 243 (4), 229 (33), 215 (10), 203 (12), 189 (35), 175 (43), 161 (54), 147 (63), 135 (75), 121 (90), 107 (93), 93 (100), 81 (73), 79 (72), 67 (67), 55 (47); HRFABMS *m/z* 272.2493 [M]$^+$ (calcd for C$_{20}$H$_{32}$, 272.2504).

(1R,3E,7E,11S,12S,14S)-14-Hydroxy-3,7,18-dolabellatriene (**5**): colorless oil; $[\alpha]_D^{20}$ +44 (*c* 0.06, CHCl$_3$); UV (CHCl$_3$) λ_{max} (log ε) 244.0 (2.48) nm; IR (thin film) ν_{max} 3370, 2936, 2360, 1290 cm^{-1}; ^{1}H NMR data, see Table 1; ^{13}C NMR data, see Table 2; EIMS 70 eV *m/z* (rel int %) 288 (5), 270 (12), 255 (22), 227 (17), 213 (12), 201 (15), 191 (38), 173 (25), 163 (41), 145 (51), 135 (76), 121 (81), 107 (94), 95 (86), 81 (100), 67 (64), 55 (69); HRFABMS *m/z* 288.2479 [M]$^+$ (calcd for C$_{20}$H$_{32}$O, 288.2453).

(1R,3E,7E,11S,12S,14S)-14-Acetoxy-3,7,18-dolabellatriene (**6**): colorless oil; $[\alpha]_D^{20}$ +29 (*c* 0.07, CHCl$_3$); UV (CHCl$_3$) λ_{max} (log ε) 241.4 (2.27) nm; IR (thin film) ν_{max} 2967, 2920, 1734, 1538 cm^{-1}; ^{1}H NMR data, see Table 1; ^{13}C NMR data, see Table 2; EIMS 70 eV *m/z* (rel int %) 330 (1), 315 (1), 288 (1), 270 (50), 255 (46), 241 (8), 227 (31), 213 (17), 201 (20), 187 (32), 173 (42), 159 (55), 145 (69), 133 (93), 119 (100), 105 (69), 91 (67), 81 (54), 67 (42), 55 (43); HRFABMS *m/z* 330.2535 [M]$^+$ (calcd for C$_{22}$H$_{34}$O$_2$, 330.2559).

(1R,3S,4S,7E,11S,12S,14S)-14-Acetoxy-3,4-epoxy-7,18-dolabelladiene (**9**): yellowish oil; $[\alpha]_D^{20}$ +47.8 (*c* 0.25, CHCl$_3$); UV (CHCl$_3$) λ_{max} (log ε) 243.0 (2.18) nm; IR (thin film) ν_{max} 2962, 2907, 1734, 1243 cm^{-1}; ^{1}H NMR data, see Table 3; ^{13}C NMR data, see Table 4; EIMS 70 eV *m/z* (rel int %) 346 (1), 328 (8), 286 (61), 271 (28), 268 (27), 253 (25), 243 (19), 228 (33), 213 (29), 201 (41), 187 (51), 173 (47), 159 (62), 145 (79), 133 (100), 119 (92), 105 (96), 91 (81), 79 (49), 67 (25), 55 (31); HRFABMS *m/z* 346.2488 [M]$^+$ (calcd for C$_{22}$H$_{34}$O$_3$, 346.2508).

(1R,3E,7S,8S,11S,12S)-7,8-Epoxy-14-oxo-3,18-dolabelladiene (**10**): colorless crystals; $[\alpha]_D^{20}$ −66.4 (*c* 0.19, CHCl$_3$); UV (CHCl$_3$) λ_{max} (log ε) 241.5 (2.24) nm; IR (thin film) ν_{max} 2966, 2925, 2859, 1733, 1457 cm^{-1}; ^{1}H NMR data, see Table 3; ^{13}C NMR data, see Table 4; EIMS 70 eV *m/z* (rel int %) 302 (39), 284 (78), 269 (41), 241 (19), 233 (14), 227 (16), 215 (31), 205 (24), 187 (57), 173 (45), 163 (92), 159 (57), 150 (58), 145 (63), 135 (90), 119 (75), 105 (94), 91 (100), 79 (69), 67 (58), 55 (50); HRFABMS *m/z* 303.2325 [M + H]$^+$ (calcd for C$_{20}$H$_{31}$O$_2$, 303.2324).

(1R,3Z,7S,8S,11S,12S)-7,8-Epoxy-14-oxo-3,18-dolabelladiene (**11**): colorless oil; $[\alpha]_D^{20}$ −13.0 (*c* 0.25, CHCl$_3$); UV (CHCl$_3$) λ_{max} (log ε) 242.5 (2.16) nm; IR (thin film) ν_{max} 2935, 1733, 1275 cm^{-1}; ^{1}H NMR data, see Table 3; ^{13}C NMR data, see Table 4; EIMS 70 eV *m/z* (rel int %) 302 (14), 284 (63), 269 (22), 256 (11), 241 (15), 215 (25), 205 (20), 187 (58), 173 (40), 163 (96), 159 (55), 150 (53), 145 (68), 135 (80), 119 (80), 105 (97), 91 (100), 79 (68), 67 (55), 55 (49); HRFABMS *m/z* 303.2330 [M + H]$^+$ (calcd for C$_{20}$H$_{31}$O$_2$, 303.2324).

(1R,3E,7E,11R,12R)-12-Hydroxy-3,7-dolabelladiene (**14**): colorless oil; $[\alpha]_D^{20}$ +16 (*c* 0.09, CHCl$_3$); UV (CHCl$_3$) λ_{max} (log ε) 242.5 (2.23) nm; IR (thin film) ν_{max} 3330, 2958, 2877, 1276 cm^{-1}; ^{1}H NMR data, see Table 3; ^{13}C NMR data, see Table 4; ^{1}H NMR (400 MHz, C$_6$D$_6$) δ 5.03 (1H, m, H-3), 5.02 (1H, m, H-7), 2.15 (1H, m, H-9a), 2.14 (1H, m, H-2a), 2.09 (2H, m, H-6), 2.05 (2H, m, H-5), 1.90 (1H, ddd, 13.8, 12.3, 1.9 Hz, H-9b), 1.80 (1H, dd, 14.9, 5.2 Hz, H-2b), 1.75 (1H, m, H-18), 1.71 (1H, m, H-10a), 1.67 (1H, m, H-11), 1.64 (1H, m, H-14a), 1.54 (1H, m, H-13a), 1.53 (3H, s, H-17), 1.46 (3H, s, H-16), 1.39 (1H, m, H-14b), 1.30 (1H, m, H-13b), 1.29 (1H, m, H-10b), 1.07 (3H, s, H-15), 0.93 (3H, d, 6.7 Hz, H-20), 0.88 (3H, d, 6.8 Hz, H-19); EIMS 70 eV *m/z* (rel int %) 290 (1), 272 (12), 257 (10), 247 (3), 229 (25), 216 (4), 201 (5), 189 (18), 175 (9), 161 (30), 149 (20), 135 (100), 121 (71), 107 (54), 93 (49), 81 (31), 67 (27), 55 (20); HRFABMS *m/z* 290.2629 [M]$^+$ (calcd for C$_{20}$H$_{34}$O, 290.2610).

(1R,2E,4R,7E,11S,12R)-2,7,18-Dolabellatriene (**15**): colorless oil; $[\alpha]_D^{20}$ −21 (*c* 0.03, CHCl$_3$); UV (CHCl$_3$) λ_{max} (log ε) 242.2 (2.53) nm; IR (thin film) ν_{max} 2948, 2920, 1538 cm^{-1}; ^{1}H NMR data, see Table 3; ^{13}C NMR data, see Table 4; EIMS 70 eV *m/z* (rel int %) 272 (32), 257 (25), 243 (5), 229 (68), 215 (10), 201 (13), 190 (25), 175 (73), 161 (47), 147 (71), 133 (60), 121 (67), 107 (100), 93 (83), 81 (74), 67 (57), 55 (50); HRFABMS *m/z* 272.2495 [M]$^+$ (calcd for C$_{20}$H$_{32}$, 272.2504).

Reduction of 2. Compound **2** (48.0 mg) was treated with NaBH$_4$ (50.0 mg) in MeOH (10 mL) and left under constant stirring at room temperature for 1 h. The reaction was quenched by the addition of H$_2$O (3 mL), and the mixture was evaporated in vacuo. The residue was purified by normal-phase HPLC, using cyclohexane/EtOAc (90:10) as eluent, to obtain **5** (7.3 mg) and **18** (31.2 mg).

(1R,3E,7E,11S,12S,14R)-14-Hydroxy-3,7,18-dolabellatriene (**18**): colorless oil; $[\alpha]_D^{20}$ +12.0 (*c* 0.10, CHCl$_3$); UV (CHCl$_3$) λ_{max} (log ε) 244.0

(2.31) nm; IR (thin film) ν_{max} 3389, 2926, 2360, 1279 cm^{-1}; ^{1}H NMR data, see Table 1; ^{13}C NMR data, see Table 2; EIMS 70 eV *m/z* (rel int %) 288 (8), 270 (14), 255 (12), 245 (6), 227 (13), 220 (14), 205 (12), 189 (21), 173 (17), 163 (56), 149 (40), 135 (79), 121 (78), 107 (92), 95 (84), 81 (100), 67 (63), 55 (70); HRFABMS *m/z* 288.2426 [M]$^+$ (calcd for C$_{20}$H$_{32}$O, 288.2453).

Epoxidation of 4. A solution of *m*-chloroperbenzoic acid (20.0 mg) in benzene (1 mL) was added dropwise to a solution of compound **4** (20.0 mg) in benzene (2 mL), and the mixture was left under constant stirring at room temperature for 30 min. The reaction was quenched by the addition of 10% Na$_2$SO$_3$ (3 mL), and the mixture was partitioned between the aqueous and the organic layer. The organic layer was washed with 5% NaHCO$_3$ and subsequently H$_2$O. After evaporation of the organic layer in vacuo, the residue was purified by normal-phase HPLC, using *n*-hexane/2-propanol (99.75:0.25) as eluent, to afford **8** (6.3 mg) and **12** (5.9 mg).

Acetylation of 5. Compound **5** (2.8 mg) was treated with Ac$_2$O (1 mL) in pyridine (1 mL) and left under constant stirring at 70 °C for 16 h. The reaction was quenched by the addition of H$_2$O (1 mL), and the mixture was evaporated in vacuo. The residue was purified by normal-phase HPLC, using cyclohexane/EtOAc (99:1) as eluent, to obtain **6** (2.3 mg).

Preparation of MTPA Derivatives of 18. Compound **18** (3.3 mg) was treated with (*R*)-MTPA chloride (5 μL) in freshly distilled dry pyridine (1 mL) and left under constant stirring at room temperature for 16 h. The reaction was quenched by the addition of H$_2$O (1 mL) and CH$_2$Cl$_2$ (3 mL), and the mixture was partitioned between the aqueous and the organic layer. After evaporation of the organic layer in vacuo, the residue was purified by normal-phase HPLC, using cyclohexane/EtOAc (95:5) as eluent, to give the (*S*)-MTPA derivative (**18a**, 3.2 mg). The (*R*)-MTPA derivative (**18b**, 2.4 mg) was prepared with (*S*)-MTPA chloride and purified in the same manner.

(S)-MTPA Derivative of 18 (**18a**): ^{1}H NMR (400 MHz, CDCl$_3$) δ 7.53 (2H, m, Ar-H), 7.39 (3H, m, Ar-H), 5.07 (1H, dd, 9.2, 6.0 Hz, H-3), 4.97 (1H, dd, 9.1, 7.1 Hz, H-14), 4.89 (1H, brs, H-20a), 4.79 (1H, dd, 9.5, 4.1 Hz, H-7), 4.66 (1H, brs, H-20b), 3.55 (3H, s, OMe), 2.65 (1H, m, H-12), 2.24 (1H, m, H-6a), 2.18 (1H, m, H-5a), 2.17 (1H, m, H-2α), 2.15 (1H, m, H-13β), 2.08 (1H, m, H-6b), 2.07 (1H, m, H-5b), 2.02 (1H, m, H-9a), 1.90 (1H, m, H-2β), 1.89 (1H, m, H-9b), 1.88 (1H, m, H-11), 1.81 (1H, m, H-13α), 1.70 (3H, s, H-19), 1.50 (3H, s, H-16), 1.47 (3H, s, H-17), 1.34 (1H, m, H-10a), 1.16 (1H, m, H-10b), 0.83 (3H, s, H-15).

(R)-MTPA Derivative of 18 (**18b**): ^{1}H NMR (400 MHz, CDCl$_3$) δ 7.51 (2H, m, Ar-H), 7.39 (3H, m, Ar-H), 5.10 (1H, dd, 9.3, 6.6 Hz, H-3), 4.92 (1H, dd, 8.9, 7.0 Hz, H-14), 4.86 (1H, brs, H-20a), 4.80 (1H, dd, 8.5, 3.7 Hz, H-7), 4.62 (1H, brs, H-20b), 3.52 (3H, s, OMe), 2.65 (1H, ddd, 13.3, 7.1, 7.1 Hz, H-12), 2.24 (1H, m, H-6a), 2.21 (1H, m, H-2α), 2.17 (1H, m, H-5a), 2.14 (1H, m, H-13β), 2.08 (1H, m, H-6b), 2.07 (1H, m, H-5b), 2.02 (1H, m, H-9a), 1.90 (1H, m, H-2β), 1.89 (1H, m, H-9b), 1.88 (1H, m, H-11), 1.68 (1H, m, H-13α), 1.67 (3H, s, H-19), 1.51 (3H, s, H-16), 1.47 (3H, s, H-17), 1.34 (1H, m, H-10a), 1.16 (1H, m, H-10b), 0.94 (3H, s, H-15).

Single-Crystal X-ray Analysis of 10. Compound **10** crystallized after slow evaporation of a saturated solution of EtOAc/CHCl$_3$ (1:1) as colorless blocks. Single-crystal X-ray diffraction data were collected at 120 K on a Nonius Kappa CCD diffractometer with graphite-monochromated Mo Kα radiation (λ = 0.71073 Å) using the Nonius Collect Software. The space group was determined on the basis of the systematic absences and confirmed by the successful structure solution and refinement. The structure was solved by direct methods and refined based on F^2 using the WINGX package. All non-hydrogen atoms were refined with anisotropic thermal parameters, whereas all hydrogen atoms were located in the calculated positions and refined in a rigid group model.

In the absence of atoms with significant anomalous scattering, the absolute configuration of **10** was indeterminate.

*Crystallographic Data of **10***: $C_{20}H_{30}O_2$, $M = 302.4$, $0.52 \times 0.24 \times 0.22$ mm, $T = 120(2)$ K, orthorhombic, space group $P2_12_12_1$ (#19) with $a = 7.7877(11)$ Å, $b = 13.9979(13)$ Å, $c = 15.5830(16)$ Å, $V = 1698.73(3)$ Å^3, $Z = 4$, $Z' = 1$, $D_{calcd} = 1.183$ Mg/m^3, $\mu = 0.074$ mm^{-1}, $F(000) = 664$, $2\theta_{max} = 55.00°$, 16 541 collected reflections, 3866 independent reflections ($R_{int} = 0.0467$), $R_1 = 0.0450$, $wR_2 = 0.0939$, GoF = 0.994 for 2997 reflections (201 parameters) with $I > 2\sigma(I)$, $R_1 = 0.0722$, $wR_2 = 0.1080$, GoF = 0.994 for all 3866 reflections, max./min. residual electron density $+0.182/-0.179$ e Å^3.

Evaluation of Antibacterial Activity. Standard strain ATCC 25923 and strain XU212, which possesses the gene encoding the TetK tetracycline efflux protein, were provided by Dr. E. Udo. Strain SA1199B, which possesses the gene encoding the NorA quinolone efflux protein, was a generous gift of Prof. G. W. Kaatz. Strain RN4220, which possesses the gene encoding the MsrA macrolide efflux protein, was provided by Dr. J. Cove. The epidemic methicillin-resistant strains EMRSA-15 and EMRSA-16 were obtained from Dr. P. Stapleton. All strains were cultured on nutrient agar and incubated for 24 h at 37 °C prior to the determination of minimum inhibitory concentration (MIC) values. Compounds **1–18** were dissolved in DMSO and subsequently diluted in Mueller-Hinton broth (MHB) to give a starting concentration of 512 μg/mL. Bacterial inocula equivalent to the 0.5 McFarland turbidity standard were prepared in normal saline for each strain and diluted to a final inoculum density of 5×10^5 cfu/mL. MHB supplemented with 10 mg/L Mg^{2+} and 20 mg/L Ca^{2+} (125 μL/well) was dispensed into wells 1–11 of each row of 96-well microtiter plates. The compound solution (125 μL) was added to the first well of each row and was serially diluted across the row, leaving well 11 empty for growth control. The final volume was dispensed into well 12, which being free of MHB or inoculum served as the sterility control. The inoculum (125 μL/well) was added to wells 1–11 of each row, and the microtiter plates were incubated for 18 h at 37 °C. The lowest concentration at which no bacterial growth was observed was recorded as the MIC. The observation was confirmed by the addition of a 5 mg/mL methanolic solution of 3-(4,5-dimethylthiazol-2-yl)-2,5-diphenyltetrazolium bromide (MTT, 20 μL/well) and further incubation for 20 min at 37 °C. Bacterial growth was indicated by a color alteration from yellow to dark blue. Norfloxacin was used as a positive control. The highest concentration of DMSO remaining after dilution (3.125% v/v) caused no inhibition of bacterial growth. All samples were tested in triplicate. Culture media were obtained from Oxoid, whereas all other chemicals were obtained from Sigma-Aldrich.

■ ASSOCIATED CONTENT

Ⓢ Supporting Information. ^{1}H and ^{13}C NMR spectra of compounds **1–18**, NOESY spectra of compounds **1–15** and **18**, NMR data in tabular form of compounds **2**, **7**, **8**, and **12**, and CIF data for the crystal structure of metabolite **10**. This material is available free of charge via the Internet at http://pubs.acs.org.

■ AUTHOR INFORMATION

Corresponding Author
*To whom correspondence should be addressed. Tel/Fax: +30-210-7274592. E-mail: roussis@pharm.uoa.gr.

Notes
$^{\perp}$Deceased on May 12, 2010.

■ ACKNOWLEDGMENT

■ REFERENCES

(1) Blunt, J. W.; Copp, B. R.; Munro, M. H. G.; Northcote, P. T.; Prinsep, M. R. *Nat. Prod. Rep.* **2010**, *27*, 165−237, and earlier reviews in this series.

(2) *MarinLit Database*; Department of Chemistry, University of Canterbury: http://www.chem.canterbury.ac.nz/marinlit/marinlit.shtml.

(3) Ioannou, E.; Quesada, A.; Vagias, C.; Roussis, V. *Tetrahedron* **2008**, *64*, 3975–3979.

(4) Ioannou, E.; Zervou, M.; Ismail, A.; Ktari, L.; Vagias, C.; Roussis, V. *Tetrahedron* **2009**, *65*, 10565–10572.

(5) Amico, V.; Oriente, G.; Piattelli, M.; Tringali, C.; Fattorusso, E.; Magno, S.; Mayol, L. *Tetrahedron* **1980**, *36*, 1409–1414.

(6) Piattelli, M.; Tringali, C.; Neri, P.; Rocco, C. *J. Nat. Prod.* **1995**, *58*, 697–704.

(7) Amico, V.; Currenti, R.; Oriente, G.; Piattelli, M.; Tringali, C. *Phytochemistry* **1981**, *20*, 848–849.

(8) Crystallographic data (excluding structure factors) for compound **11** have been deposited with the Cambridge Crystallographic Data Centre as supplementary publication no. CCDC 759848. Copies of the data can be obtained, free of charge, on application to CCDC, 12 Union Road, Cambridge CB2 1EZ, UK (fax: +44-(0)1223-336033 or e-mail: deposit@ccdc.cam.ac.uk).

(9) Duran, R.; Zubia, E.; Ortega, M. J.; Salva, J. *Tetrahedron* **1997**, *53*, 8675–8688.

(10) Seco, J. M.; Quiñoá, E.; Riguera, R. *Chem. Rev.* **2004**, *104*, 17–117.

(11) Ireland, C.; Faulkner, D. J. *J. Org. Chem.* **1977**, *42*, 3157–3162.

(12) Ramírez, M. C.; Toscano, R. A.; Arnason, J.; Omar, S.; Cerda-García-Rojas, C. M.; Mata, R. *Tetrahedron* **2000**, *56*, 5085–5091.

(13) Wang, Y.; Harrison, L. J.; Tan, B. C. *Tetrahedron* **2009**, *65*, 4035–4043.